Transport properties of $Nd_{1.2}Ba_{1.8}Cu_3O_Z$ ultrathin films by field-effect doping

M. Salluzzo,* A. Cassinese, G. M. De Luca, A. Gambardella,† A. Prigiobbo, and R. Vaglio

INFM-COHERENTIA and Dipartimento di Scienze Fisiche, Università di Napoli "Federico II" Piazzale Tecchio 80, I-80125 Napoli, Italy

(Received 9 July 2004; published 30 December 2004)

We report a study on the transport properties of ultrathin $Nd_{1.2}Ba_{1.8}Cu_3O_z$ (NdBCO) films by using field effect devices. Very high quality NdBCO films, having thickness ranging between 5 and 130 nm, have been prepared using diode high oxygen pressure sputtering. The temperature dependence of the resistivity has been studied as a function of the number of layers and of doping induced by field effect. An insulating-superconducting transition is observed in these films when the thickness is increased above 9 unit cells (u.c.). Below 9 u.c. the resistivity follows a 2D Mott variable range hopping temperature dependence and the localization length, estimated from a fit, is found to increase when holes are injected in the sample by field effect. A similar trend is observed when the number of layers in the film increases as a result of the changes of doping. The analysis suggests that hole density plays a major role in the transport properties of NdBCO ultrathin films.

DOI: 10.1103/PhysRevB.70.214528 PACS number(s): 74.72.−h, 74.62.Dh, 74.25.Fy

I. INTRODUCTION

Superconducting-insulator (S-I) transition in the high critical temperature superconductors (HTS) family is one of the most interesting issues in condensed matter physics.[1] There are different ways to induce a S-I transition in an optimally doped superconducting compound. For example, it is possible to change the composition by cation substitution or by modifying the oxygen concentration. The change in composition alters the holes doping, but inexorably modifies the structure and introduces chemical disorder in the system.

The temperature versus holes doping phase diagram seems to be a general feature of the HTS, suggesting that density of carriers in the CuO_2 planes plays a major role in the electronic properties of these materials.[2] However, there is no agreement on this subject, since other parameters may affect both the normal and the superconducting state properties of HTS. For example, a correlation between the critical temperature and the Cu–O–Cu buckling angle have been found in polycrystalline $(La_{1-x}Ca_x)(Ba_{1.75-x}La_{0.25+x})Cu_3O_y$ samples having different doping levels.[3] Furthermore, the effect of external uniaxial pressure on the critical temperature of several HTS compounds[4] suggests that crystalline structure deformations may have a major role in determining the electronic properties of these materials. Some theoretical papers[5] have shown that a relevant role on the properties of the CuO_2 planes is played by the ratio between the Madelung potentials at the apical oxygen (above the CuO_2 plane) and the one at the planar oxygen (in the CuO_2 plane). This ratio can be modified not only by hole doping, but also by changes in the structure and by cation substitution. Consequently, studies on the role of chemical doping on the transport properties of HTS cannot discriminate between the effects associated with modification of holes distribution in CuO_2 planes and the structural ones. In this perspective, the use of the electric field effect to modify the density of carriers in a thin layer of an HTS film seems extremely attractive. Field effect devices (FED) made of metal transition oxides and HTS thin films can be used to modify the number of carriers in a layer of thickness equal to the Thomas–Fermi screening length λ_{TF} (of the order of one unit cell). This can be done without introducing chemical disorder or modifying the structure. Considerable field effect modulation of the magnetoresistance was demonstrated in $La_{0.9}Ca_{0.1}MnO_3$ films,[6] while modifications of the critical temperature of superconducting samples was achieved in field effect experiments on optimally doped $Nd_1Ba_2Cu_3O_{7-\delta}$ (Ref. 7) and overdoped $Y_{0.7}Ca_{0.3}Ba_2Cu_3O_y$ (Ref. 8) films.

Recently the authors have demonstrated that a strong modulation of the conductivity can be induced by field effect in insulating $Nd_{1.2}Ba_{1.8}Cu_3O_z$ (NdBCO) thin films.[9] An apparent insulating-superconducting transition has been observed in one of the eight unit cells (u.c.) device tested. In this paper we present a detailed study of the transport properties of the $Nd_{1.2}Ba_{1.8}Cu_3O_z$ (NdBCO) thin films as a function of field effect doping. The analysis of these results provides experimental evidence that underdoped NdBCO films, having doping close to the I-S transition, behave as 2D Mott variable range hopping insulators and the localization of the carriers, associated to the change of hole density, determines and consequently modifies the transport properties.

II. DEVICE PREPARATION AND CHARACTERIZATION

Field effect devices were fabricated fully "*in situ*" following the design sketched in Fig. 1(a). A NdBCO film is grown on a $10\times10\times0.5$ mm^3 $SrTiO_3$ (1 0 0) (STO) substrate on which 15 nm thin Au contacts, a 150 nm Al_2O_3 insulating film, and the Au gate electrode are sequentially deposited "*in situ*" using suitable stencil-steel masks.

The Al_2O_3 film is deposited by dc magnetron reactive sputtering using a pure aluminum target in a mixture of Ar (flux of 50 sccm) and O_2 (4 sccm) gas. The deposition conditions have been adjusted in order to have stoichiometric or oxygen rich films according to Ref. 10. As shown in Fig. 1(b), the sputtering voltage has a characteristic dependence

 ©2004 The American Physical Society

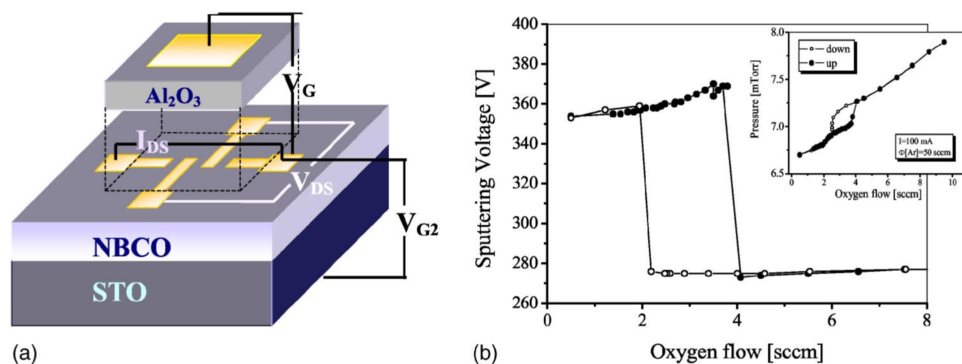

FIG. 1. (a) Sketch of the field effect device used in this work. (b) Typical sputtering voltage versus oxygen flux calibration performed at 100 mA of sputtering current before the deposition of the Al_2O_3 dielectric film; in the inset the absolute pressure versus oxygen flux is also shown.

on the oxygen flux: when the Al-target surface layer becomes completely oxidized, a sudden voltage drop occurs corresponding to the switching to a sputtering regime characterized by a negligible deposition rate. In order to have a useful rate and to grow oxygen rich Al_2O_3 film, the maximum oxygen flux before the sudden voltage drop occurs is chosen. With a sputtering current of 100 mA and a total pressure of 10 Pa, a growth rate of about $0.04\ \mathrm{nm \cdot s^{-1}}$ is typically obtained. The breakdown field of our Al_2O_3 films is in the range of 7×10^6 V/cm. The resistivity across the Al_2O_3 layer is larger than $10^4\ \Omega \cdot m$ up to a field of 4×10^6 V/cm.

The $Nd_{1.2}Ba_{1.8}Cu_3O_z$ films were grown by high oxygen pressure diode sputtering from a single target at 230 Pa using a mixture of 95% of oxygen and 5% argon as sputtering gas, a target to substrate distance of 15 mm, and a deposition temperature, referred to here as the heater temperature, of 1120 K. The composition was measured by EDX (energy dispersive x-ray) analyses. X-ray diffraction measurements, performed by a conventional three circles CuK_α diffractometer, show that the NdBCO samples are untwinned and tetragonal up to 70 unit cells. The very high quality of the structure of these films is clearly confirmed by the full width at half maximum (FWHM) of the rocking curves measured on symmetric as well as asymmetric reflections: this width is 0.03° on the (001) peak and lower than 0.10° on (005) and (308) peaks. Reflectivity oscillations, merging with Pendellösung fringes present around the (001) reflection (Fig. 2), are observed for films having thickness even larger than 80 nm, demonstrating very smooth surfaces and structural coherence extended along the whole thickness. The number of unit cells can be consequently measured by x-ray diffraction with a precision of one unit cell (u.c.). The surface of $Nd_{1.2}Ba_{1.8}Cu_3O_z$ thin films is composed by a two levels terrace structure, with steps typically 0.4 nm high. The root mean square roughness, measured on $5 \times 5\ \mu m^2$ area, is below 1 nm for 100 nm thick films and 0.4 nm for 10 nm thin films.[11]

Gold layers are grown by a thermal Joule effect evaporator source. The contacts are 50 μm wide and 20 nm thin, the distance between the current pads [I_{DS} in Fig. 1(a)] is about 200 μm, and the drain to source channel length [V_{DS} in Fig. 1(a)] is 25 μm[9]. Resistivity was measured as a function of temperature, at different gate voltages, using a four-probe technique, where a constant current (between 1 to 10 μA) is injected between the current pads and the drain-source voltage drop is acquired. Only in the case of 4 u.c. films the measurements have been performed with a two-probes technique, by applying a voltage difference between drain and source and measuring the current with a Keitley 487 picoammeter. In order to assure that the properties of the NdBCO films were not modified by the deposition of other layers on their surfaces, the resistivities of twin samples were also measured as a function of the temperature using a standard Van der Pauw method.

The average number of carriers of our films was evaluated by Seebeck effect measurements. The well established correlation[12] between the room temperature value, S_{290}, and the number of holes per CuO_2 planes, p_{pl}, provides a rapid method for the determination of the carriers density as a function of the thickness. All cuprates, both in form of polycrystalline, epitaxial films and crystals, obey to this relationship.[12] Deviations are observed in the case of $Y_1Ba_2Cu_3O_{7-\delta}$ due to substantial contribution provided by the Cu(1)O oxygen chains. In our films, instead, long chains are evidently destroyed by the Nd/Ba substitution, since these films are tetragonal; therefore the relationship between S_{290} and p_{pl} gives a reliable estimation of the hole density.

III. EXPERIMENTAL RESULTS

In Fig. 3 the resistivity versus temperature of NdBCO films, having thickness ranging between 4 and 116 unit cells, is shown. It is clear that a superconducting-insulator transi-

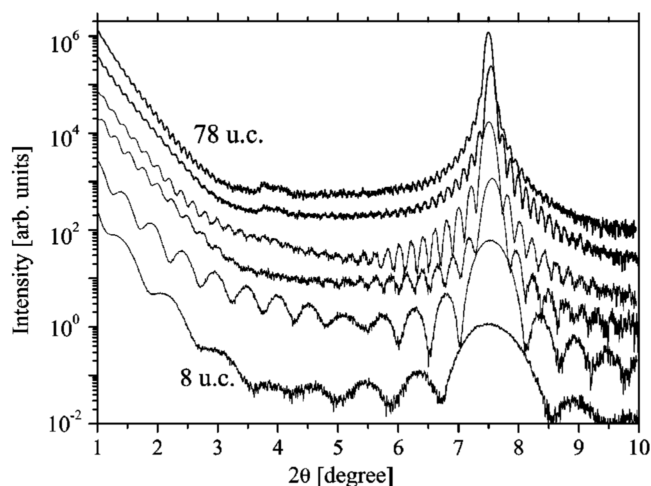

FIG. 2. Low angle $\vartheta - 2\vartheta$ diffraction spectra measured on 8, 14, 29, 38, 60 and 78 u.c NdBCO films. Each scan has been displaced by a fixed offset for clarity.

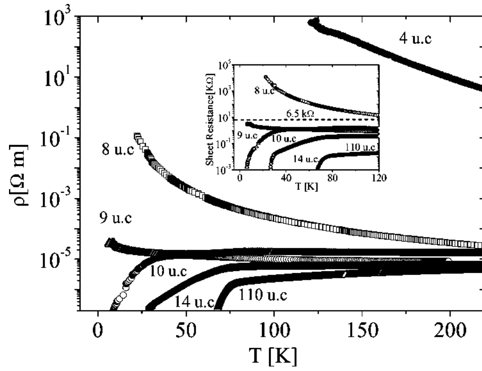

FIG. 3. Temperature dependence of the resistivity in NdBCO films characterized by different thickness as indicated in the figure. In the inset the data are shown as sheet resistance versus temperature, showing that the superconducting-insulating transition appears at values of $R^{\square}$ lower than R_Q.

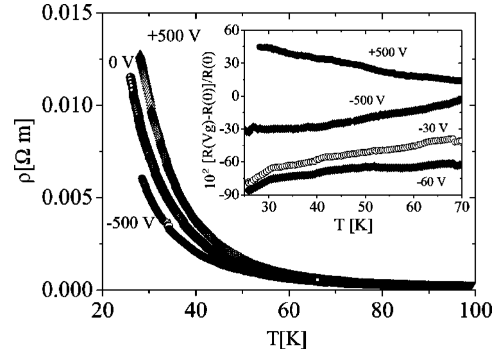

FIG. 5. Temperature dependence of the resistivity in an 8 u.c. FED as a function of the gate voltage applied through the $SrTiO_3$ substrate used as dielectric. In the inset the relative change of the channel resistance obtained with the gate voltage applied through the $SrTiO_3$ ($Vg=-500$ V, open diamonds; $Vg=+500$ V, filled diamonds) and through the Al_2O_3 layer for comparison (at -30 and -60 V) are shown.

tion takes place when the thickness is reduced below 9 unit cells. All the samples below this thickness exhibit insulating ($d\rho/dT<0$) temperature dependence of the resistivity and no superconductivity down to 4.2 K. The thickness dependence of the resistivity can be associated to the effect of strain induced by the different structure of the $SrTiO_3$ substrate and of the $Nd_{1.2}Ba_{1.8}Cu_3O_z$ film. An analysis of the correlations between structure and transport properties of NdBCO is beyond the scope of this paper and will be reported elsewhere. We wish only to mention that thin $Nd_{1.2}Ba_{1.8}Cu_3O_z$ films (thickness lower than 70 u.c.) are tetragonal and almost perfectly in plane matched with the $SrTiO_3$ substrate. Consequently our films are strained, since bulk $Nd_{1.2}Ba_{1.8}Cu_3O_z$ samples are orthorhombic with $a=0.387(0)$ nm and $b=0.391(0)$ nm.[13] As shown in Fig. 3, the 8–9 u.c. samples are at boundary between the insulating and the superconducting behavior, therefore small changes in the average thickness or in the oxygen content can significantly affect the conductivity. The number of carriers of 8 u.c. films, determined from the Seebeck coefficient, is about 0.05 holes per CuO_2 plane, in agreement with the I-S transition expected by the phenomenological phase diagram of cuprates. We note that the superconducting-insulating transition appears at values of the sheet resistance $R^{\square}$ lower than the universal value $R_Q=h/4e^2=6.48\ k\Omega$, as shown in the inset of Fig. 3.

Hole doping by field effect is demonstrated in Fig. 4, where the resistance versus temperature of 4 and 8 unit cells films is plotted for several gate voltages. Applying a negative voltage to the gate, a decrease of the resistivity was observed for all devices, demonstrating that mobile carriers are holes, as expected. In this geometry, a gate voltage of 10 V corresponds to an electric field of about 0.7×10^6 V/cm. The corresponding injected surface carrier density is estimated to be in the range of 4×10^{12} cm^{-2}. The number of holes per CuO_2 plane is $p_{pl}=0.05$ in an 8 u.c. film; consequently, with the hypothesis that holes are injected in the first unit cell and completely transferred to the CuO_2 planes by field effect, a change from $p_{pl}=0.05$ to $p_{pl}=0.06$ is expected applying a gate voltage of about -30 V $\{p_{pl}(Vg=-30\text{ V})=p_{pl}(Vg=0)+\Delta n_s/2\times area_{CuO_2}=0.05+[1.2\times10^{13}\text{ cm}^{-2}/2\times(0.3905\times10^{-7}\text{ cm})^2]\}$. Field effect modulation of the conductivity is also obtained by applying the field through the 0.5 mm thick $SrTiO_3$ substrate used as dielectric. The very high dielectric constant of the STO makes it possible to observe effects even if the applied electric field is very low due to the large substrate thickness. In Fig. 5 the temperature dependence of the resistivity in an 8 u.c. film is shown in function of the gate voltage. Note that much larger gate voltages are in this case necessary to observe any effect. Here the charges are injected primarily in the first layer of the deposited film at the interface with the substrate. The effect for positive and negative voltages again demonstrates that for injecting holes a decrease of the resistivity is clearly observed at temperatures lower than 50 K. Moreover, the percentage change of the resistivity (inset of Fig. 5) is similar for both field polarities.

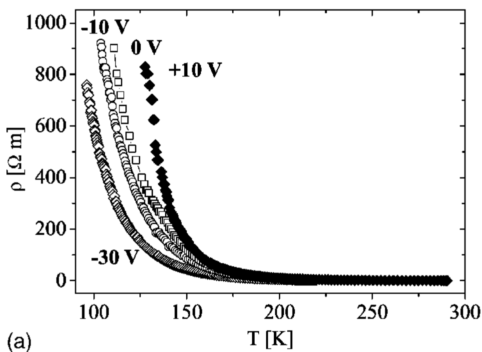

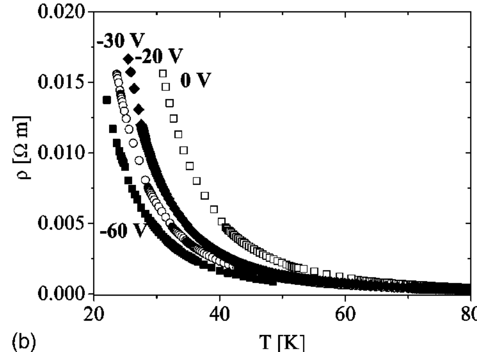

FIG. 4. Temperature dependence of the resistivity in 4 and 8 u.c. FED measured for different values of the gate voltage: (a) 4 u.c. FED at $Vg=0$ V (open squares), $Vg=+10$ V (filled diamond), $Vg=-10$ V (open circles), $Vg=-30$ V (open diamonds); (b) 8 u.c. FED at $Vg=0$ V (open squares), $Vg=-20$ V (filled diamond), $Vg=-30$ V (open circles), $Vg=-60$ V (closed squares).

Since the dielectric constant of the $SrTiO_3$ is a function of the field and of the temperature, these data can be only qualitatively analyzed.

IV. ANALYSIS OF THE EXPERIMENTAL RESULTS

The variable range hopping (VRH) model is commonly used to describe the transport mechanism in strongly electron-correlated insulating materials.[14,15] In this scenario, conduction of carriers takes place by hopping between lattice sites, where they are localized within a given localization length d.[14] In the original derivation by Mott, the conduction mechanism was described as a phonon assisted tunneling hopping. In the case of electron-correlated material the transport mechanism has a different origin, nevertheless the Mott derivation of the conductivity is still valid if the Coulomb interaction between the carriers is not taken into account. Efros–Shklovlskii (E-S) showed that in some systems the Coulomb repulsion could not be neglected at low temperature and in this case the density of states becomes gapped at the Fermi surface[16] (while in the Mott theory it is considered constant). A crossover from a Mott regime to an E-S regime is expected at low temperature in this case. It can be shown that, for both Mott and E-S models, a simple analytical expression for the temperature dependence of the resistivity can be derived:[17]

$$\rho(T) = \rho_1\left(\frac{T}{T_0}\right)^{2\alpha} \exp\left[\left(\frac{T_0}{T}\right)^{\alpha}\right]. \quad (1)$$

Here $\alpha=\frac{1}{2}$, $\frac{1}{3}$, or $\frac{1}{4}$ in the case of E-S, 2D or 3D Mott models, respectively, and T_0 is a characteristic temperature that assumes different functional expressions depending on the model. In spite of its simplicity, the analytical expression for the resistivity (1) is astonishingly general. Similar equations are obtained including in the calculation multiple hopping processes.[18] Moreover Eq. (1) remains valid when the conduction is associated with hopping of polarons.[19]

In the Mott theory the characteristic temperature T_0 depends on the localization length d and on the density of states at the Fermi energy g_{E_f}. For a 2D system $T_0 = \beta/(g_{E_f}^{2D}\cdot k_B \cdot d^2)$. Levin *et al.*,[20] using a percolation approach, have demonstrated that $\beta=14$. This value is in good agreement with numerical simulation.[21]

In the E-S model the characteristic temperature T_0 depends on the localization length and it is not a function of the density of states at Fermi level, but of the dielectric susceptibility κ of the material. Again for the 2D system it can be shown that $T_0=6.2\, e^2/(k_B\kappa d)$ in the E-S theory.

The comparison between the different models (Mott 2D, Mott 3D, and E-S) and the experimental results for an 8 u.c. film (data taken at zero gate voltage) is shown in Fig. 6. It is clear that the Mott 2D law reproduces the experimental results with good accuracy in a large temperature range. This result is valid also for the other 8 u.c. insulating NdBCO films. Consequently the Mott 2D model gives the best agreement with the experimental results.

In Fig. 7 the experimental data on the resistivity of an 8 u.c. FED, plotted now in log-scale at different gate voltages, are shown. While either Mott 2D or E-S models can describe the low temperature behavior at the different doping levels, major deviations from the E-S law are observed at high temperatures. The main effect of doping by field effect is the change of the characteristic temperature T_0 that systematically decreases raising the density of holes. The localization lengths of this 8 u.c. FED, estimated using the T_0 values found by fitting the data with the Mott 2D and E-S models, are plotted in the insets of Fig. 7. For the calculations we used a density of states of 1×10^{14} states eV^{-1} cm^{-2} (Ref. 22) and $\kappa=26$.[23] In both cases the localization length is of the order of 3 or 4 in plane lattice constants, lower than the typical values of the superconducting coherence length in this compound (1.8 to 2.0 nm corresponding to about $5a$, with $a=0.39$ nm). Even assuming a density of states of 0.5×10^{14} states eV^{-1} cm^{-2}, the localization length, obtained by the Mott 2D model, remains lower than 2.5 nm.

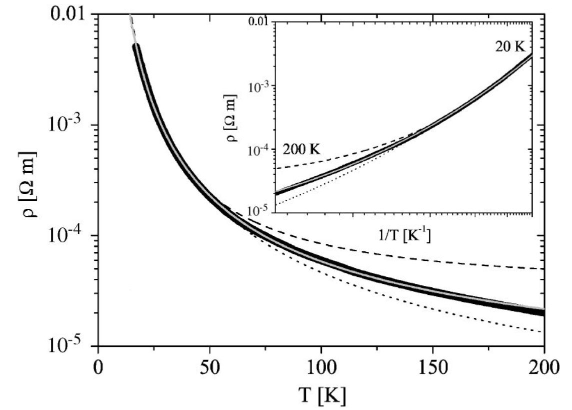

FIG. 6. Comparison between the experimental resistivity data on an 8 u.c. film (at zero gate voltage, black filled circles) and the fit obtained with different theoretical models: Mott 2D (gray continuous line), Mott 3D (dot line), E-S (dashed line). In the inset the data are plotted as resistivity in function of $1/T$ on a log-log scale.

Similar results are obtained in the case of other insulating NdBCO films. In Fig. 8(a) we plot data of NdBCO films of 4, 8, and 10 unit cells. Data for two 8 u.c. films are shown, and one of them exhibits an I-S transition by field effect. From the inset one can see that the localization length increases exponentially when the thickness is larger than 8 u.c., approaching the limit where the VRH model is no more valid.

A similar analysis, in function of field effect doping, was carried out for the data regarding the 8 u.c. FED exhibiting I-S transition. As shown in Fig. 8(b), the slope of the experimental data in the normal state decreases by applying negative voltages. The localization length is found to change from 2.0 to 2.8 nm. It is worth noting that 2.0 nm is roughly the maximum values of d reached by the other 8 u.c. FET still non-superconducting, (see Fig. 7) at maximum hole doping.

V. DISCUSSION

The experimental results suggest that NdBCO thin films with thickness lower than 10 u.c. are 2D Mott-VRH insulators, and that the insulating behavior is driven by localization

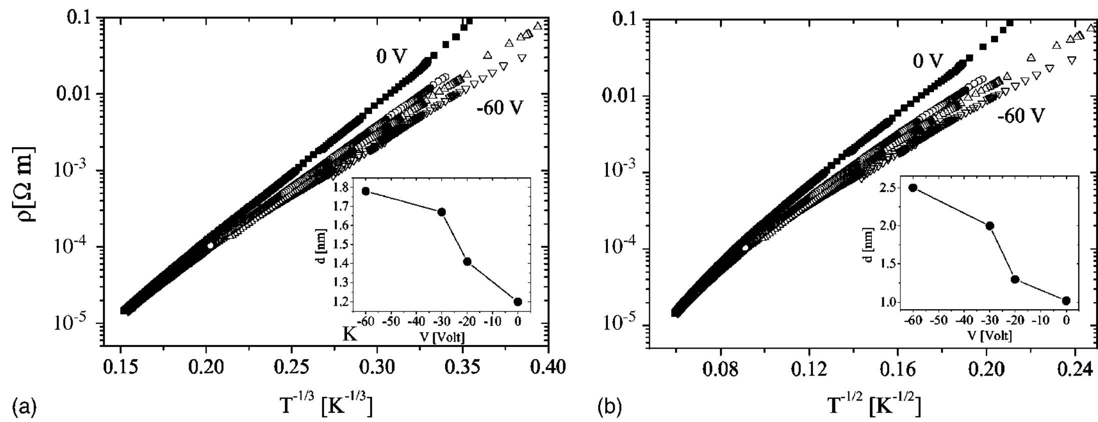

FIG. 7. Experimental data on 8 u.c. FED as a function of $T^{-1/3}$ (a) and $T^{-1/2}$ (b) at 0, −20, −30, and −60 V gate voltages. In the insets the localization lengths, obtained from a fit using MOTT 2D (a) and E-S (b) models, are shown.

of carriers. Field effect doping modifies the localization length in a manner consistent with transport provided by holes, i.e., d increases by increasing hole doping. The localization length is also found to be a function of film thickness, decreasing with the number of unit cells that composes the film. Both results can be explained supposing that the hole density, changed by field effect or by the film thickness, is responsible for the observed transport properties.

The localization length was found to be a function of the Pr doping in Pr-doped compounds, like $Y_{1-x}Pr_xBa_2Cu_3O_7$,[24] $Gd_1Pr_xBa_{2-x}Cu_3O_7$,[25] and $Tl_2Ba_2Ca_{1-x}Pr_xCu_2O_y$,[26] where the Pr content modifies both the T_c and the hole doping in the optimally doped 123 and 2212 families. In these materials the hole localization has been attributed to the Pr ions that may affect the properties of the CuO_2 planes in different ways, i.e., by changing the Pr valence to the 4+ state (due to the presence of $4f$ orbitals), by introducing disorder, or by modifying the oxygen content. It turns out that Pr doping always modifies the number of hole carriers present in the CuO_2 planes. By comparing these results with our experimental data, we arrive at the conclusion that hole doping is the key ingredient in determining the transport properties of strongly underdoped compounds. It is worth noting that the values of the localization length determined in Refs. 25 and 26 for non-superconducting Pr-doped compounds is around 2.0 nm, a value very similar to that found in insulating NdBCO 8 u.c. films. In our opinion these results give strong hints that the localization of the carriers in the CuO_2 plane is mainly associated to hole doping, that is modified, in these different systems, by field effect, by Pr substitution, or by strain-related effects in very thin films. Incidentally we note that superconducting to insulating transition is observed in samples where the carriers are localized within a distance smaller than the coherence length. These results are consistent with the changes of the localization lengths with the applied gate voltage in our 8 u.c. FED exhibiting the I-S transition. Since changes in the transport properties are obtained in the same sample by applying the field, we can rule out that the chemical or structural disorder plays any role.

The similarity between the effect of chemical doping and field effect doping, however, must be considered with some care, due to the intrinsic differences among the two kinds of doping. First of all, our analysis assumed implicitly that, in field effect doped samples, holes are injected homogeneously along the whole thickness.This assumption is clearly invalid if the preexisting carriers are able to screen the electric field

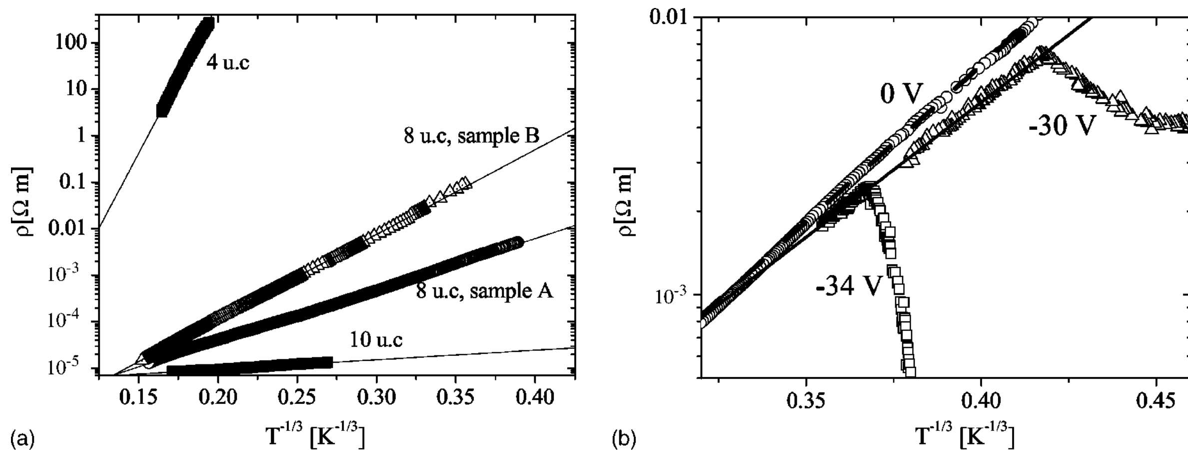

FIG. 8. (a) Resistivity versus $T^{-1/3}$ data in function of the number of unit cells for 4, 8, and 10 u.c. FED. Continuous lines guides for eyes; (b) resistivity versus $T^{-1/3}$ for 8 u.c. sample A FED exhibiting a field effect induced insulating to superconducting transition. The continuous line is the fit obtained at −30 and −34 V gate voltage using the MOTT 2D models, while the dashed line is the fit at 0 gate voltage.

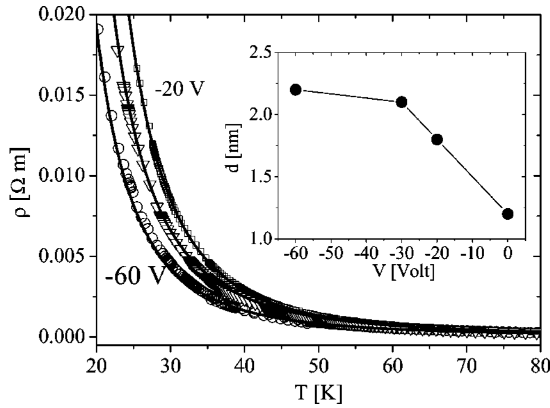

FIG. 9. Comparison between the experimental data on sample B FED and the fit obtained using Eq. (5).

within the Thomas–Fermi length, i.e., in the first unit cell for the HTS. It is not clear if Thomas–Fermi model can be really applied to strongly underdoped (in fact insulating) and layered HTS. However, it is important to verify if and how our analysis presented above would be modified. If the field effect influences the properties of a surface portion of the film, the measured resistivity is composed by the parallel contribution between the doped layer and the bulk. In this case we can write the sample conductivity as follows:

$$\sigma(T) = \frac{t}{\lambda_{TF}\rho_s(T)} + \frac{t}{(t-\lambda_{TF})\cdot\rho_{bulk}(T)}, \quad (2)$$

where t is the film thickness, and $\rho_s(T)$ and $\rho_{bulk}(T)$ are the contributions coming from the field effect doped surface and the bulk, respectively, whose temperature dependence is assumed to follow Eq. (4) with $\alpha=\frac{1}{3}$ (2D-Mott). $\rho_{bulk}(T)$ is determined by fitting the data at *zero* gate voltage, while λ_{TF} is assumed to be 1 u.c. In Fig. 9 the comparison between the experimental data for the 8 u.c. FED [see Fig. 4(b)] and the fit obtained from Eq. (2) are shown. The fit is extremely good in the full temperature range, though there is no real improvement with respect to the simple 2D-Mott model that still explains our data with irrelevant changes in the fitting parameters. The localization length, plotted in the inset of Fig. 9, is only slightly larger than the one determined from the previous fit [Fig. 7(b)]. Consequently the main conclusions drawn by the simplified analysis are essentially confirmed.

Another related point is the intrinsic difference between hole injection and hole depletion. Since the field penetrates only in the first unit cell of the film, it would be simpler to observe field effect modulation by injecting holes in the sample (that decreases the resistivity of the surface layer). This seems to be not the case in our samples as clearly shown by the data in Fig. 6 for an 8 u.c. film where the field effect seems to be of the same order of magnitude for positive or negative applied gate voltages. Moreover, data on 4 u.c. films [Fig. 4(a)], where the bulk contribution to the conductivity has a lower weight compared to the 8 u.c. FEDs, show that hole depletion gives rise to a stronger change of the resistivity than hole injection. This result is not completely understood, but they may be explained taking into account that the relation between resistivity, or localization length, and doping is not linear and it may be possible that a injection or depletion of holes is in reality not symmetric.

Finally, it is interesting to compare our results to related data reported in the literature. Field effect doping on YBCO underdoped films was reported in Refs. 27 and 28, where field effect devices were made of a 50 nm thick insulating YBCO grown sequentially on an insulating STO used as dielectric. The whole structure is deposited on a conducting Nb-doped STO substrate used as gate electrode. In this case the field is applied through the STO film. An analysis of the transport properties of YBCO insulating films was employed in the framework of the VRH mechanisms of conduction. A crossover between the Mott 2D and the E-S limits were reported in function of the temperature for some of their devices. We have not found a similar crossover in our samples in function of doping and of the number of layers. We think that there are two possible explanations for such differences. The first one relies on the fact that our resistivity versus temperature data are acquired with a temperature independent amount of holes injected, since the Al_2O_3 layer has a temperature independent dielectric constant. This is different from the data reported in Ref. 28, because the STO dielectric constant is strongly temperature dependent. Second, we use thinner films, consequently the contribution of the field effect undoped layer is very small if compared to the case of 50 nm thick YBCO film.

In conclusion, we studied the transport properties of NdBCO having different numbers of unit cells and we modified the conductivity of the samples by field effect doping. Analysis of the data in the framework of the VRH models shows that a 2D Mott model reproduces the temperature dependence of the resistivity on insulating thin films (thickness lower than 9 u.c.) and that the localization length d increases both with the film thickness and by increasing the hole density using field effect. Comparison of our data with experimental results obtained on chemically Pr doped compounds reveals that Pr doping, strain induced modification of hole density, and field effect doping have a similar effect on the transport properties of Mott-VRH insulating HTS compounds, providing a further indication that the carrier density plays a major role in the properties of these compounds.

ACKNOWLEDGMENTS

The authors are grateful to Professor M. Putti, Dr. D. Marrè, and M. Tropeano for the Seebeck effect measurements. Professor A. Barone is gratefully acknowledged for discussions and suggestions on data interpretation.

*Corresponding author. Email address: salluzzo@na.infn.it
†Present address: INFM-S3 and Department of Physics, University of Modena, via Campi 213/A, I-41100, Modena, Italy.

[1] M. Imada, A. Fujimori, and Y. Tokura, Rev. Mod. Phys. **70**, 1039 (1998).
[2] J. B. Torrance, Y. Tokura, A. I. Nazzal, A. Bezinge, T. C. Huang, and S. S. P. Parkin, Phys. Rev. Lett. **61**, 1127 (1988); Y. Ando, Y. Hanaki, S. Ono, T. Murayama, K. Segawa, N. Miyamoto, and S. Komiya, Phys. Rev. B **61**, R14956 (2000).
[3] O. Chmaissem, J. D. Jorgensen, S. Short, A. Knizhnik, Y. Eckstein, and H. Shaked, Nature (London) **397**, 45 (1999).
[4] X. J. Chen, H. Q. Lin, and C. D. Gong, Phys. Rev. Lett. **85**, 2180 (2000).
[5] Y. Ohta, T. Tohyama, and S. Maekawa, Phys. Rev. B **43**, 2968 (1991); X. J. Chen and H. Q. Lin, *ibid.* **69**, 104518 (2004).
[6] H. Tanaka, J. Zhang, and T. Kawai, Phys. Rev. Lett. **88**, 027204 (2002).
[7] D. Matthey, S. Gariglio, and J. M. Triscone, Appl. Phys. Lett. **83**, 3758 (2003).
[8] G. Yu. Logvenov, A. Sawa, C. W. Schneider, and J. Mannhart, Appl. Phys. Lett. **83**, 3528 (2003).
[9] A. Cassinese, G. M. DeLuca, A. Prigiobbo, M. Salluzzo, and R. Vaglio, Appl. Phys. Lett. **84**, 3933 (2004).
[10] M. Kharrazi Olsson, K. Macák, U. Helmersson, and B. Hjörvarsson, J. Vac. Sci. Technol. A **16**, 639 (1998).
[11] G. M. De Luca, G. Ausanio, M. Salluzzo and R. Vaglio, Proceedings of the 6th European Applied Conference on Superconductivity, Sorrento, Italy (2003).
[12] J. L. Tallon, J. R. Cooper, P. S. I. P. N. de Silva, G. V. M. Williams, and J. W. Loram, Phys. Rev. Lett. **75**, 4114 (1995).
[13] E. Goodilin, M. Limonov, A. Panfilov, N. Khasanova, A. Oka, S. Tajima, and Y. Shiohara, Physica C **300**, 250 (1998).
[14] N. F. Mott, J. Non-Cryst. Solids **1**, 1 (1968).
[15] N. F. Mott and E. A. Davis, *Electronic Processes in Non-Crystalline Materials*, 2nd ed. (Oxford U. P., London, 1979).
[16] A. L. Efros and B. I. Shklovskii, J. Phys. C **8**, L49 (1975).
[17] R. Mansfield, in *Hopping Transport in Solids*, edited by M. Pollak and B. I. Shklovskii (North-Holland, Amsterdam, 1991).
[18] A. Perez-Garrido, M. Ortuno, E. Cuevas, J. Ruiz, and M. Pollak, Phys. Rev. B **55**, R8630 (1997) and references therein.
[19] M. Foygel, R. D. Morris, and A. G. Petukhov, Phys. Rev. B **67**, 134205 (2003).
[20] E. I. Levin, V. L. Nguyen, B. I. Shklovskii, and A. L. Efros, Sov. Phys. JETP **65**, 842 (1987).
[21] D. N. Tsigankov and A. L. Efros, Phys. Rev. Lett. **88**, 176602 (2002).
[22] W. E. Pickett, Rev. Mod. Phys. **61**, 433 (1989).
[23] J. Clayhold *et al.*, Phys. Rev. B **39**, 777 (1989).
[24] G. A. Levin, T. Stein, C. C. Almasan, S. H. Han, D. A. Gajewski, and M. B. Maple, Phys. Rev. Lett. **80**, 841 (1998).
[25] M. R. Mohammadizadeh and M. Akhavan, Eur. Phys. J. B **33**, 381 (2003).
[26] S. N. Bhatia, P. Chowdhury, S. Gupta, and B. D. Padalia, Phys. Rev. B **66**, 214523 (2002).
[27] T. Doderer, C. C. Tsuei, W. Hwang, and D. M. Newns, Phys. Rev. B **62**, 5984 (2000).
[28] F. P. Milliken, T. Doderer, R. H. Koch, and C. C. Tsuei, Phys. Rev. B **62**, 9143 (2000).